Arabian Journal of Chemistry (2023) **16**, 104791

King Saud University

Arabian Journal of Chemistry

www.ksu.edu.sa
www.sciencedirect.com

ORIGINAL ARTICLE

An efficient two-step approach for the preparative separation and purification of eight polyphenols from *Hibiscus manihot* L. flower with high-speed countercurrent chromatography

Ju-Zhao Liu [a,1], Le-Le Wen [a,1], Xiao-Li Tian [a,1], Yu-Jie Fu [b], Qi Cui [a,*]

[a] *College of Pharmaceutical Science, Zhejiang Chinese Medical University, Hangzhou 311402, PR China*
[b] *College of Biological Sciences and Technology, Beijing Forestry University, No. 35, Tsinghua East Road, Haidian District, Beijing 100083, PR China*

Received 31 January 2023; accepted 4 March 2023
Available online 14 March 2023

KEYWORDS

Hibiscus manihot L. flowers;
High-speed countercurrent chromatography;
Polyphenols;
Preparative separation;
Ultrasonic-assisted extraction;
Molecular docking

Abstract In the present study, a green and efficient ultrasonic-assisted extraction method of polyphenols from *Hibiscus manihot* L. flowers (HMLF) was performed, and the corresponding experimental parameters were optimized by Taguchi OA Design. Meanwhile, a two-step high-speed counter-current chromatography coupled with macroporous resin was successfully established with the optimal two-phase solvent systems comprising EtOAc-MeOH-H_2O (100:3:100, v/v/v) and Hex-EtOAc-MeOH-H_2O (1:5:1:5, v/v/v/v) to isolate and prepare eight polyphenols with purities exceeding 95%, including two phenolic acids and six flavonoids, respectively. The yield of the isolated polyphenols was determined to be 50.4 mg from the enriched extract in a single run. Moreover, the interactions of the eight isolated compounds with AChE and BuChE were explicitly evaluated and described by molecular docking. This study confirms that the proposed method is a cost-effective and powerful strategy for the scaled-up extraction and preparative separation of the high-purity polyphenols from HMLF, and provides an opportunity for automation and systematic preparation of natural products used in the food and pharmaceutical industries.

1. Introduction

Hibiscus manihot L. flowers (HMLF, Fig. 1) are applied for food and functional supplements because of the high nutritional and economic merits of polyphenols and other secondary products (Liu et al., 2022a). In our previous studies, phenolic acids and flavonoids were found to be the main polyphenols in HMLF, which possessed antioxidant, anti-inflammatory, antimicrobial, cardioprotective, and neuroprotective activities, etc. (Gebicki & Nauser, 2021; Huang et al.,

* Corresponding author.
E-mail address: zcmucq@163.com (Q. Cui).
[1] These authors contributed equally to this work.

Peer review under responsibility of King Saud University.

Production and hosting by Elsevier

https://doi.org/10.1016/j.arabjc.2023.104791
1878-5352

Fig. 1 The plant of *Hibiscus manihot* L. flower.

2022; Albini et al., 2021; Xu et al., 2021). Neurodegenerative diseases are one of the major diseases that severely threaten human health, the most common of which is Alzheimer's disease (AD). AD is associated with the selective loss of cholinergic neurons in the brain as well as a drop in acetylcholine levels. A useful therapeutic therapy for AD is to stimulate the cholinergic function by inhibiting cholinesterase function, including acetylcholinesterase (AChE) and butyrylcholinesterase (BuChE), which are considered effective candidates for AD treatment (Vrabec et al., 2022). Meanwhile, some bioactive compounds in HMLF, such as hibifolin, have been shown to prevent β-amyloid (Aβ) induced cell death, implying that it may be a potential novel treatment for neurodegenerative diseases (Temerk and Ibrahim, 2016; Zhu et al., 2007; Zhu et al., 2009). Numerous studies have demonstrated that frequent consumption of chlorogenic acid and caffeic acid in daily meals can assist in neuroprotection as well as ameliorate cognitive function (Socala et al., 2021; Alam et al., 2022; Annunziata et al., 2021). Also, the potential roles of these polyphenols have sparked great interests globally, such as the antimicrobial properties in the ongoing global antimicrobial resistance crisis, and it is worth exploring the polyphenol-rich HMLF. Whereas, a small number of other substances in the crude extract of polyphenols limited the application of these active ingredients. Consequently, the exploitation of an effective approach is essential for improving the separation efficiency and purity of polyphenols.

Many techniques are utilized to extract polyphenols and other natural products, such as conventional solvent extraction, heat reflux extraction, microwave-assisted extraction (MAE) and ultrasonic-assisted extraction (UAE), etc. (Sridhar et al., 2021; Li et al., 2021; Gonzalez-Rivera et al., 2021). Non-conventional extraction methods, including MAE and UAE, are frequently applied for the extraction of natural products (Sridhar et al., 2021). Compared with conventional extraction methods, MAE has the advantages of short extraction time and high extraction efficiency, but it is not suitable for heat-resistant natural active ingredients and is only appropriate for short extraction time, making it challenging for large-scale manufacturing (Périno-Issartier et al., 2011). UAE is simple and easy to operate with low consumption of solvent and energy. The instantaneous temperature rise caused by the absorption of ultrasonic sound energy in plant materials has no effect on the structure or biological activity of polyphenols, and the secondary effect of ultrasonic is conducive to plant components dissolving (Liu et al., 2022c). Because of shorter residence durations between particles and medium, the use of tiny quantities of material and the fewest solvents, and enhanced yields in total polyphenol extraction, UAE was deemed the most effective technique for extracting polyphenols from plant matrix (Yang et al., 2021; Jovanović et al., 2022). Ultrasonic cavitation could destroy the plant cell wall and cell membrane, facilitate the mass transfer, and promote the release of polyphenols into the extraction solution, thus improving the extraction efficiency (Christou, Stavrou & Kapnissi-Christodoulou, 2021; Wu et al., 2021; Liang et al., 2019; Souadia, Gourine, & Yousfi, 2022). UAE technology was selected as the preferred extraction method to extract HMLF polyphenols due to the above advantages.

In general, active ingredients were isolated from plant materials by a multi-step liquid–liquid extraction followed by the separation and purification of the monomeric compounds in the extract by different chromatographic separation methods. However, these methods have inevitable drawbacks, such as time-, labor- and resource-intensive, potential sample denaturation and irreversible sample adsorption (Jiang et al., 2022). High-speed counter-current chromatography (HSCCC) is an efficient liquid–liquid partition chromatography technology that not only overcomes the shortcomings of traditional chromatographic column separation but also facilitates the rapid and large-scale preparation of target compounds (Dermiki, Garrard & Jauregi, 2021; Zuo et al., 2019; Wang et al., 2019). It has been widespread application in isolating and purifying bioactive compounds from natural plants (Lin et al., 2020; Song et al., 2020; Xue et al., 2021; Yang et al., 2020; Zhang et al., 2021). The partition coefficient (K) of analytes is commonly used to evaluate the separation effect of HSCCC, and an adequate two-phase solvent system (TPSS) is critical to the triumphant separation of various components (Friesen et al., 2015). Therefore, when provided with a suitable solvent system, HSCCC may serve as a powerful alternative development strategy workflow for the isolation and purification of natural products, as well as have tremendous potential for technical applications in the manufacturing of high-value-added products.

The goals of this work were to: (1) optimize the extraction conditions for the UAE of HMLF polyphenols by Taguchi OA Design (TOAD); (2) screen the best macroporous resin for polyphenols enrichment by studying static, dynamic adsorption and desorption experiments; (3) establish a cost-effective and credible HSCCC separation approach for the preparation of HMLF polyphenols using suitable two-phase solvent systems; (4) identify the target compounds with ESI-MS/MS, ^{1}H NMR and ^{13}C NMR spectroscopy; (5) predict the AChE and BuChE inhibitory potentials of the isolated compounds by molecular docking technique (Fig. 2). The established feasible strategy serves as a guide for separating and purifying high-purity natural compounds, as well as demonstrating the potential of this method in the large-scale preparation of active ingredients.

2. Materials and methods

2.1. Plant materials and chemicals

HMLF was collected (Heilongjiang Province, China, northern latitude 45°43′9″, east longitude 126°38′5″), shade dried with

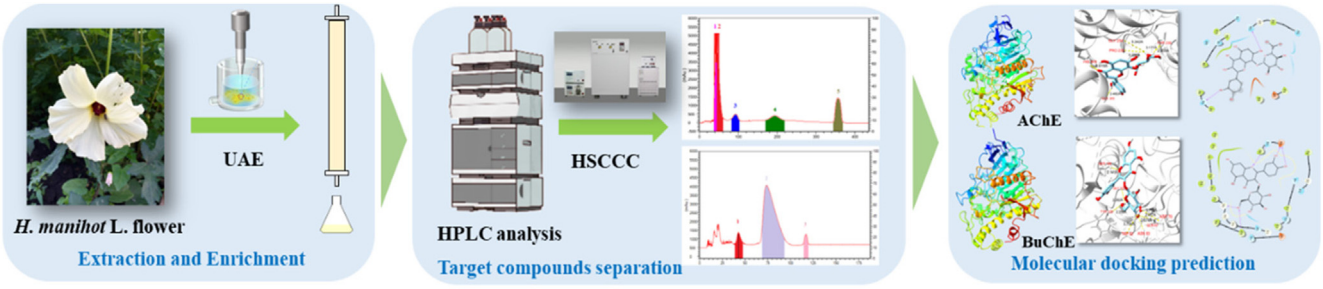

Fig. 2 Schematic illustration of the workflow for the extraction, enrichment, separation and molecular docking predictions of isolated compounds in HMLF.

final moisture of 3.54%, pulverized (360 μm) and stored at room temperature. All standard items (≥98%), ACN (≥99.9%) and H_3PO_4 (85–90%) of HPLC grade used for HPLC were purchased from Sigma-Aldrich.

2.2. Preparation of crude extract

In a conical flask, 2 g of HMLF was extracted with a certain concentration of ethanol solution using ultrasonic-assisted extraction (UAE) in an ultrasonic bath (XM-500UVF, Kunshan, China). In the UAE, the parameters included liquid/solid ratio, extraction time, extraction temperature, ultrasonic power and ethanol concentration at four levels, which were methodically optimized by Taguchi OA Design (TOAD) to determine the effect of individual factors on the response variable of the total flavonoid content (Table 1). Under the optimal conditions, 1000 g of HMLF samples were extracted, concentrated and suspended in water for macroporous adsorption resin experiments. All experiments were performed in triplicate.

2.3. Enrichment of chemical compositions by macroporous adsorption resin

Static adsorption and desorption experiments were implemented as follows: The pretreated resins (1.0 g of dry resin, Shanghai Yuanye Biotechnology Co. LTD, China, Table S1) were weighed and combined with the sample solution (60 mL) in a 150 mL Erlenmeyer flask, which was then shaken and adsorbed for 6 h in a constant temperature shaker (25 ℃) at 100 rpm. When the adsorption equilibrium was achieved, the resins were filtered out of the solution and the concentrations of the target compounds were determined by HPLC. Subsequently, 60 mL of 60% ethanol was added to the separated resins for desorption at 100 rpm for 6 h. The remaining step was the same as before, with HPLC analysis being used to identify the desorption solution.

The 24 mL sample solution passed down the glass column (1.5 × 50 cm) wet-packed with 5 g (dry weight) of resin at a fixed flow rate of 3 BV/h, and the effluent was gathered and monitored at 1 BV intervals. After attaining adsorption equilibrium, the column was in turn eluted with ultrapure water and 3 BV different ethanol solutions (10%, 20%, 30%, 40%, 50%, 60%, 70%, 80%, 90%, 100%), and the results were monitored and analyzed. The enriched sample was eventually obtained for further preparative separation of target compounds by HSCCC.

2.4. Separation and purification of target compounds from HMLF by HSCCC

2.4.1. Measurement of partition coefficients

The TBE-300C HSCCC instrument (Tauto, Shanghai, China), equipped with three coil separation columns (total capacity of 0.3 L) and a sample loop of 20 mL, was applied to separate and purify target compounds from HMLF. An appropriate amount of the sample produced by Section 2.3 was dissolved in a 10 mL tube with the prepared TPSS and permitted to fully equilibrate. Then the separated upper and lower phases were evaporated and dissolved in chromatographic methanol for HPLC analysis using the same equipment and method specified by Cui et al. (2020) to identify the appropriate TPSS by measuring the K value and separation factor (α) of the compounds to be separated. The determination of target compounds was implemented with an Agilent 1200 HPLC system coupled with an Agilent 1200 multiple wavelength detector. Chromatographic separation was carried out on a KYA TECH HIQ Sil column (250 mm × 4.6 mm, 5 μm). At 30 ℃ and 1 mL/min, the elution sequence with 0.5% H_3PO_4 solution (A) and ACN (B) was as follows: 0–40 min, 90–83% A; 40–59 min, 83–67% A; 59–62 min, 67% A; 62–65 min, 67–90% A. The HPLC chromatograms of CHA, CAA, and RU, HY, ISQ, HI, QOR, QOG were detected at a wavelength of 330 nm and 254 nm, respectively.

2.4.2. Preparation of TPSS and sample solution

The preferred solvent system was placed in a 2000 mL separating funnel and then shaken vigorously. After the phase separation, the upper and lower phases of ultrasonic degassing were classified as stationary and mobile phases, respectively. The preparation of the sample solution was to disperse the enriched sample obtained in Section 2.3 in a solvent mixture composed of 5 mL of each of the stationary and mobile phases.

2.4.3. Separation procedure

The stationary and mobile phases were successively pumped into the HSCCC system at a flow rate of 50 mL/min and 2 mL/min, respectively. The sample solution to be separated was injected into the injection valve when the system attained hydrodynamic equilibrium, and the eluent was then continu-

Table 1 Taguchi OA Design and ANOVA for the total flavonoid content.

Runs	Factors					TFC (RE mg/g DW)[f]
	A (L[a], mL/g)	B (T[b], min)	C (Temp[c], ℃)	D (UP[d], W)	E (EC[e], %)	
1	1 (10)	1 (10)	1 (20)	1 (200)	1 (50)	40.883
2	1 (10)	2 (20)	2 (30)	2 (300)	2 (60)	45.447
3	1 (10)	3 (30)	3 (40)	3 (400)	3 (70)	50.998
4	1 (10)	4 (40)	4 (50)	4 (500)	4 (80)	47.038
5	2 (20)	1 (10)	2 (30)	2 (300)	4 (80)	54.983
6	2 (20)	2 (20)	1 (20)	1 (200)	3 (70)	43.291
7	2 (20)	3 (30)	4 (50)	4 (500)	2 (60)	61.476
8	2 (20)	4 (40)	3 (40)	3 (400)	1 (50)	59.595
9	3 (30)	1 (10)	3 (40)	4 (500)	2 (60)	70.651
10	3 (30)	2 (20)	4 (50)	3 (400)	1 (50)	64.681
11	3 (30)	3 (30)	1 (20)	2 (300)	4 (80)	56.148
12	3 (30)	4 (40)	2 (30)	1 (200)	3 (70)	58.633
13	4 (40)	1 (10)	4 (50)	2 (300)	3 (70)	61.515
14	4 (40)	2 (20)	3 (40)	1 (200)	4 (80)	57.715
15	4 (40)	3 (30)	2 (30)	4 (500)	1 (50)	66.684
16	4 (40)	4 (40)	1 (20)	3 (400)	2 (60)	59.765
Source	A	B	C	D	E	
DF	3	3	3	3	3	
Seq-SS	685.331	76.903	227.573	20.339	98.424	
Adj-SS	685.331	76.903	227.573	20.339	98.424	
Adj-MS	228.444	25.634	75.857	6.780	32.808	
F-value	33.695	3.781	11.189	1.000	1.839	
p-value	< 0.05	> 0.05	< 0.05	> 0.05	> 0.05	
Level-1	46.091	57.008	50.022	54.677	57.961	
Level-2	54.836	52.783	56.437	55.676	59.335	
Level-3	62.528	58.826	59.740	57.607	53.609	
Level-4	61.420	56.258	58.677	56.916	53.971	
Delta	16.437	6.043	9.718	2.930	5.726	
Rank	1	3	2	5	4	

[a] Liquid/solid ratio (mL/g);
[b] Extraction time (min);
[c] Extraction temperature (℃);
[d] Ultrasonic power (W);
[e] Ethanol concentration (%); [f] Total flavonoid content (RE mg/g DW); Seq-SS, Sequential sum of the square; Adj-SS, Adjacent sum of the square; Adj-MS, Adjacent sum of the mean square.

ously monitored at 254 nm. Fractions were collected manually based on UV absorption and concentrated under a vacuum before HPLC detection.

2.5. Total flavonoid content

The total flavonoid content (TFC) of the samples was calculated and represented as grams of rutin equivalents per 1 g of the extract (RE mg/g extract, $y = 0.6756x + 0.0111$, $R^2 = 0.9991$) as described in our prior work (Liu et al., 2022a).

2.6. Structural identification

ESI-MS/MS, FT-IR, ^1H and ^{13}C NMR were used to structurally identify the isolated compounds with the Agilent 6460 Accurate-Mass (Agilent Technologies, CA, USA), Thermo Fisher Nicolet iS50 Fourier transform infrared spectrometer (Thermo Fisher Technologies, USA) and Bruker 500 MHz spectrometer (Bruker BioSpin Corporation, Billerica, MA).

2.7. Molecular docking

The molecular docking procedures of the isolated compounds against AChE and BuChE were performed with AutoDock Vina to investigate the binding mode of ligands with the receptors. The crystal structures of AChE (PDB ID; 3LII) and BuChE (PDB ID; 6ESJ) were obtained from the protein data bank (Dvir et al., 2010; Rosenberry et al., 2017). Before docking, the ligands and receptors were dehydrated, hydrogenated, charged, and saved in PDBQT format. In docking calculation, the receptor was considered semi-flexible while the ligand was flexible, and the grid matrix of the docking region was scaled to guarantee full coverage of the protein molecule (Liu et al., 2022c). The grids were set to (74, 74, 72) and (108, 112, 104), and the docking centers were (82.170, 89.554, −9.450) and (0, −10, −20) for AChE and BuChE, respectively. The best score with the suitable energetically favored conformations was applied for further analysis. The interaction of the isolated compounds with amino acid residues of AChE and BuChE

was analyzed and represented using ChimeraX and Maestro 11.5.

2.8. Statistical analysis

Analysis of variance (ANOVA) was performed to confirm whether the process parameters are statistically significant to TFC using MINITAB 17. $p < 0.05$ was considered as statistically significant.

3. Results and discussions

3.1. Optimization of the conditions for extracting HMLF

The extraction parameters for TFC in HMLF were determined methodically by TOAD. To examine the influence of individual parameters on the TFC response variable (Table 1), five control factors with a total of four levels were chosen as the independent variables in TOAD: liquid/solid ratio (A), extrac-

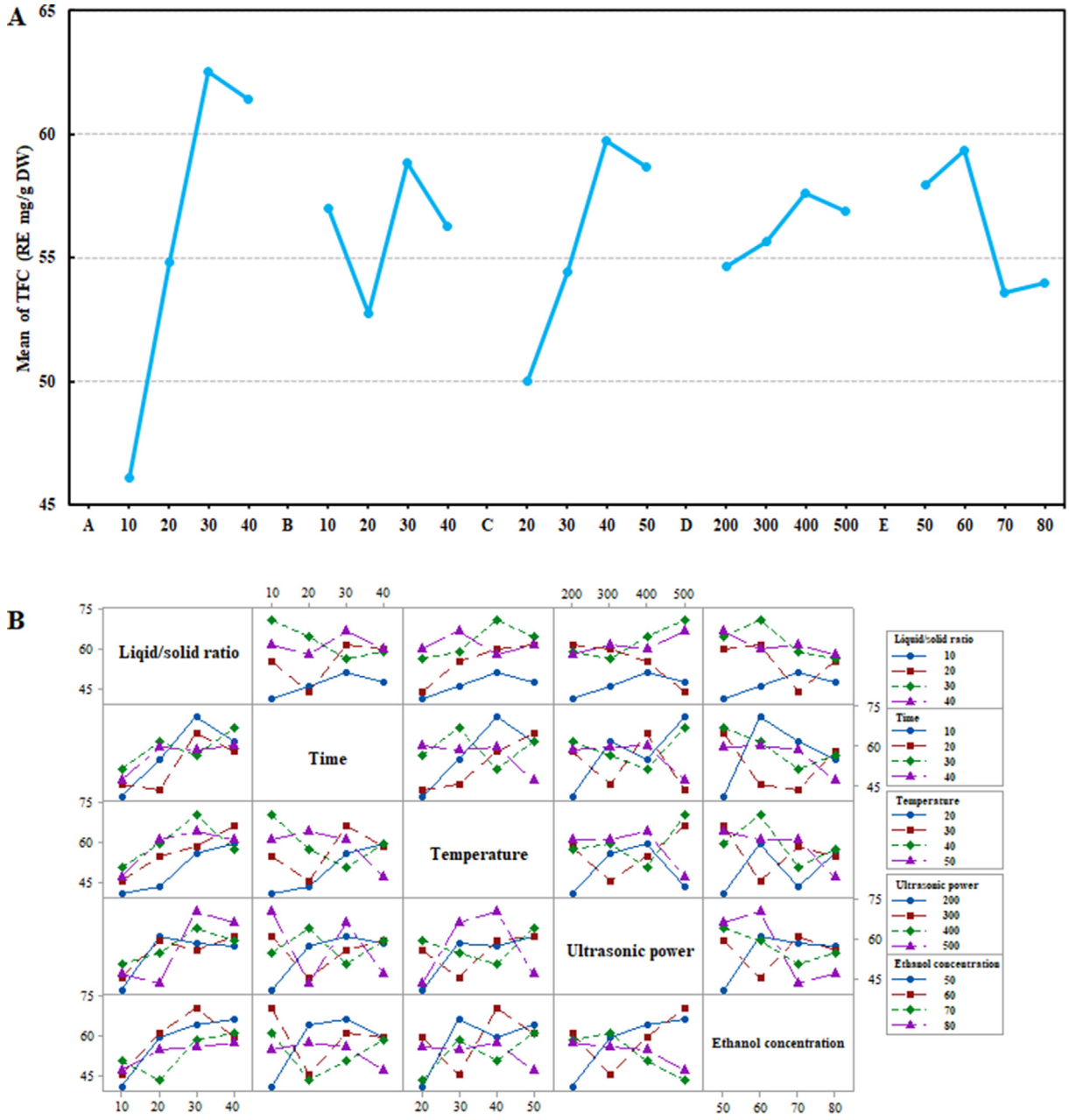

Fig. 3 Main effects plot for the mean of TFC (A) and interaction plot for TFC (B) in HMLF by Taguchi OA Design (TOAD) experiments; and A-E in the main effects for the mean of TFC represents Liquid/solid ratio (mL/g), Extraction time (min), Extraction temperature (℃), Ultrasonic power (W), Ethanol concentration (%).

tion time (B), extraction temperature (C), ultrasonic power (D) and ethanol concentration (E). An analysis of variance (ANOVA) was carried out to determine whether the technical parameters were statistically significant using MINITAB 17. Fig. 3A depicted the main effect of the five variables, in which the X- and Y-axes reflected the selection range of each variable and the mean of TFC. It can be discovered that the main effect of the factor increased as the slope of the line connecting the specified ranges increased. This finding was statistically represented in Table 1 as the rank of the main effects of each of the identified factors. The *F*-value for each parameter reveals which parameter significantly affects TFC, and the higher the *F*-value, the more significant the factor. In Table 1, the liquid/solid ratio exhibited the highest *F*-value, with extraction temperature ranking second. The *p*-values of the factors were used to decide the statistical significance of the terms (Razmi et al., 2022). There was a statistically significant relationship between the TFC and the variables since the *p*-values for liquid/solid ratio and extraction temperature were less than 0.05. While there was no statistically significant relationship between the other three variables and TFC. The ranking of a factor's main effect increased with its delta value (Tan et al., 2022), which conformed to the graphical analysis of the interaction illustrated in Fig. 3B. The ranks were liquid/solid ratio, extraction temperature, extraction temperature, ethanol concentration and ultrasonic power, in descending order. From the Pareto chart of five extraction parameters in Fig. S1A-E, it can be found that the influence on TFC was as follows: A_3- > C_3 > E_2 > B_3 > D_3. Among them, liquid/solid ratio, extraction temperature, ethanol concentration and extraction time possessed a superior influence on TFC, which was basically consistent with the results in Table 1. Therefore, the maximal TFC of 70.653 RE mg/g DW was obtained by using 60% ethanol with a liquid/solid ratio of 30 mL/g at 40 ℃ and 400 W of ultrasonic power for 30 min ($A_3B_3C_3D_3E_2$) by verification experiment.

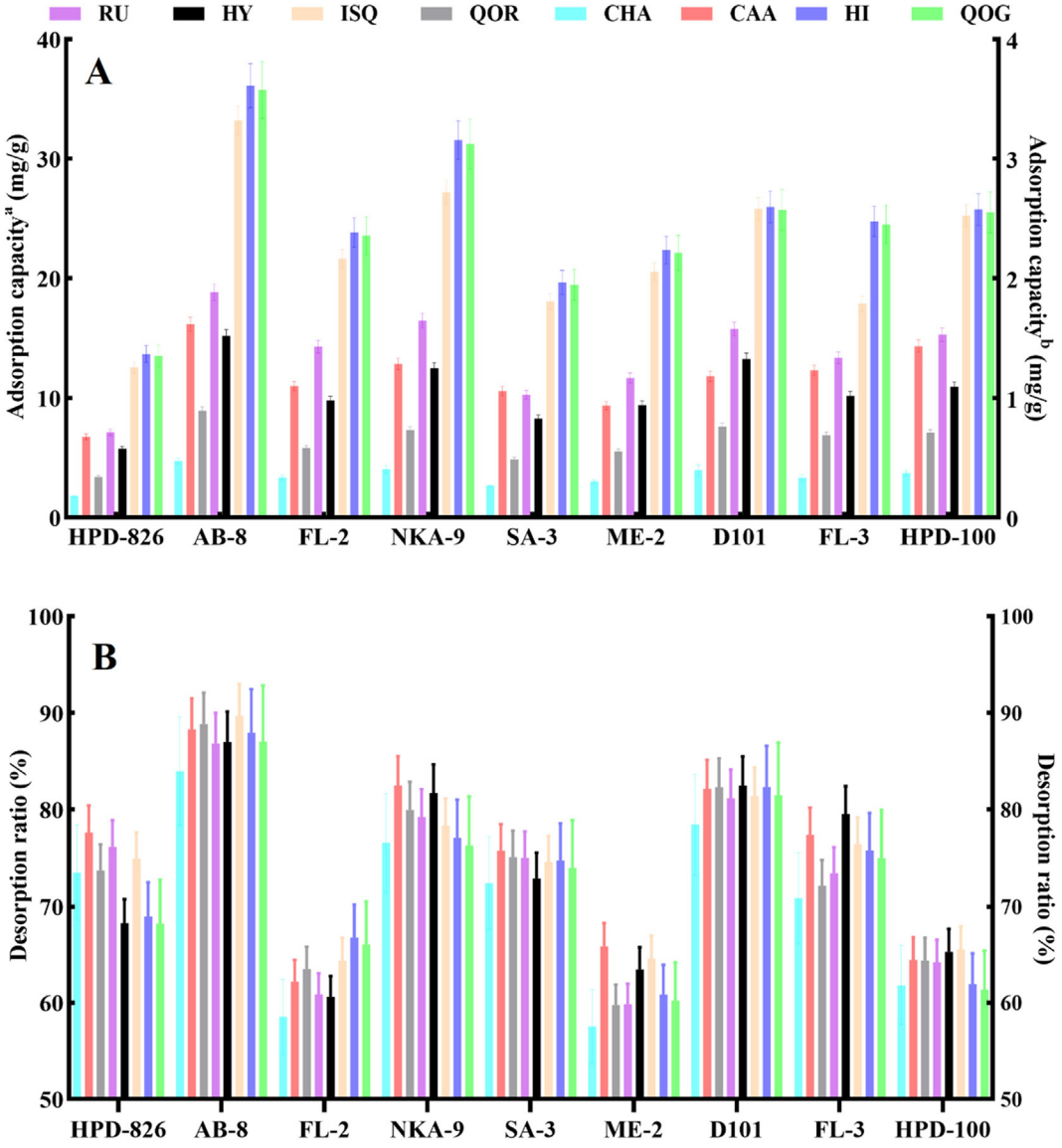

Fig. 4 Adsorption capacity (A) and desorption ratio (B) of RU, HY, ISQ, QOR, CHA, CAA, HI and QOG using nine different macroporous resins.

3.2. Preparation of the chemical compositions enriched by macroporous adsorption resin

Nine macroporous resins were evaluated for the absorption and desorption performances of chemical compositions from HMLF. It was discovered that weak-polar AB-8 resin exhibited better performance than others (Fig. 4A and B). Also, the parameters of the resin including feed volume and elution conditions, were optimized by a dynamic desorption experiment. The corresponding feed volumes for the chemical com-

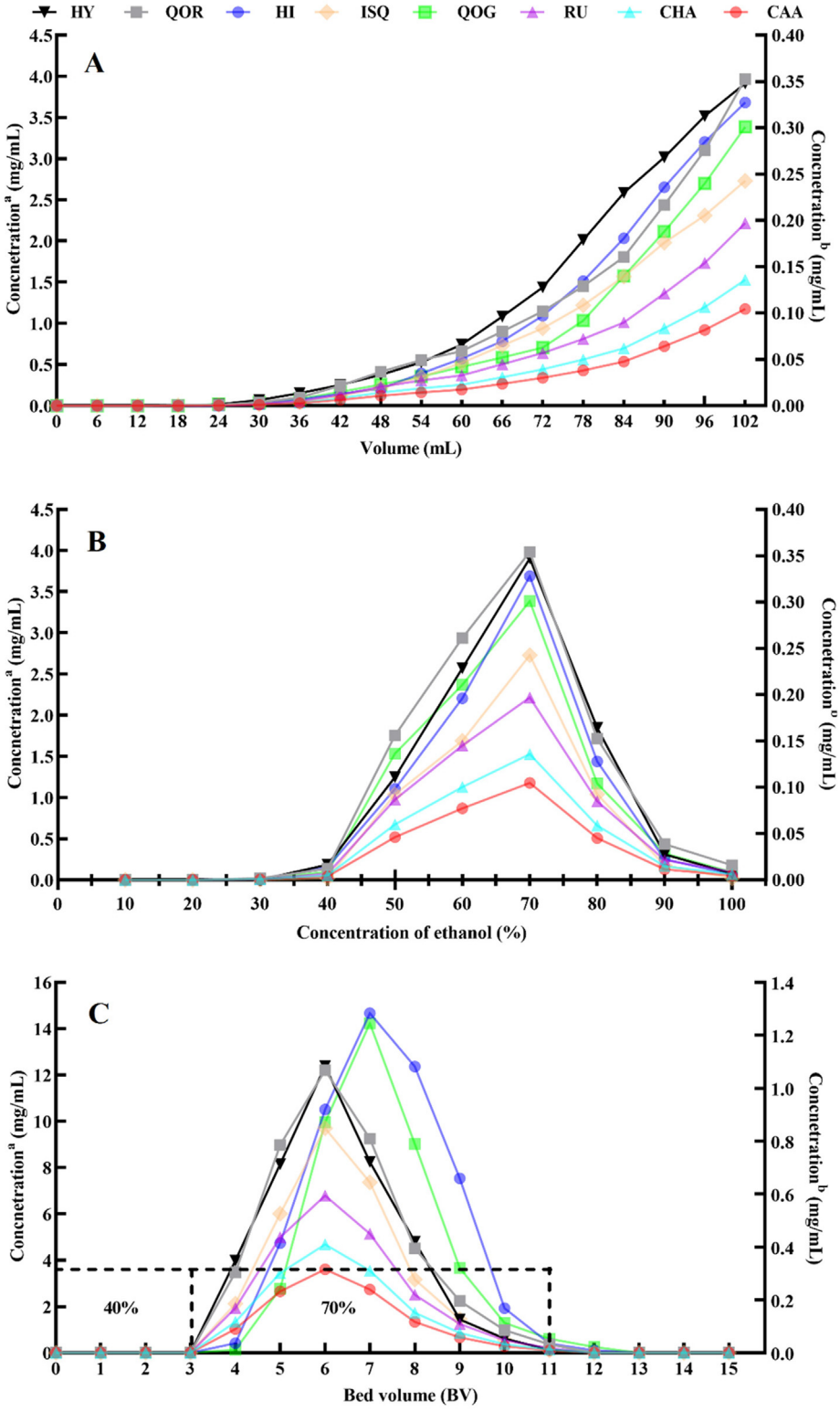

Fig. 5 Dynamic breakthrough curves (A), dynamic desorption curves (B) and profile of desorption of RU, HY, ISQ, QOR, CHA, CAA, HI and QOG (C). (A-C) [a] Concentration of HY, ISQ and HI, [b] Concentration of RU, QOR, CHA, CAA and QOG.

positions on AB-8 resin were 9/4 BV, 9/4 BV, 7/3 BV, 7/3 BV, 7/3 BV, 7/3 BV, 8/3 BV and 8/3 BV, respectively. Considering all the target chemicals, a 3 BV sample solution on AB-8 resin was chosen for dynamic adsorption (Fig. 5A). As shown in Fig. 5B, the target compounds were hardly desorbed before 40% ethanol. The desorption rates of target chemicals rose

Table 2 K values of the target compound in different TPSS.

Solvent system	Volume ratio	K_1	K_2	K_3	K_4	K_5	K_6	K_7	K_8
Hex-EtOAc-MeOH-H_2O	2:5:2:5	0.052	0.074	0.049	0.065	0.082	0.085	0.057	0.258
Hex-EtOAc-MeOH-H_2O	1:5:1:5	0.224	0.359	0.218	0.273	0.363	0.399	0.304	1.317
EtOAc-MeOH-H_2O	4:2:5	0.261	0.153	2.268	0.325	0.237	3.935	3.901	0.084
EtOAc-MeOH-H_2O	100:15:100	0.193	0.157	0.079	0.082	0.283	0.652	1.542	0.403
EtOAc-MeOH-H_2O	100:10:100	0.582	0.552	1.006	0.042	0.187	0.072	0.664	0.172
EtOAc-MeOH-H_2O	100:6:100	2.856	2.331	1.657	0.560	3.233	3.175	2.020	8.571
EtOAc-MeOH-H_2O	100:4:100	1.135	1.862	2.348	2.785	1.475	1.802	1.200	3.983
EtOAc-MeOH-H_2O	100:3:100	0.803	1.729	0.487	1.004	1.673	1.687	0.915	1.038
EtOAc-MeOH-H_2O	100:2:100	0.661	0.975	0.702	0.668	3.733	3.679	1.846	13.995
EtOAc-*n*-Butanol-H_2O	4:1:5	0.163	0.275	0.198	8.114	13.061	12.186	4.806	29.157
Hex-$CHCl_3$-MeOH-H_2O	3:6:6:4	0.619	0.647	0.226	0.198	11.941	11.137	14.308	10.477

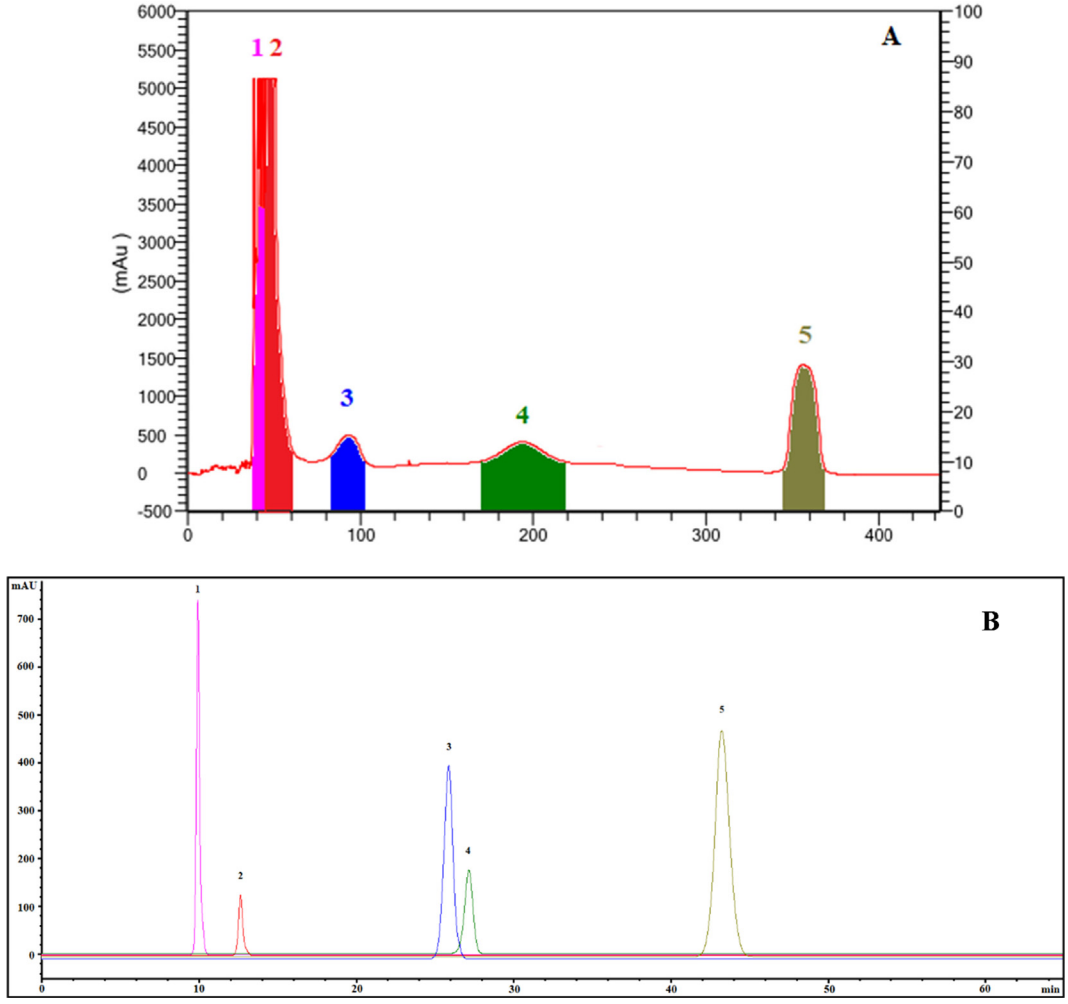

Fig. 6 HSCCC chromatogram of five target compounds isolated from HMLF (A) and HPLC chromatogram of five HSCCC fractions (B). 1, CHA; 2, CAA; 3, QOR; 4, RU; 5, HI. For HSCCC, solvent system: EtOAc-MeOH-H_2O (100:3:100, v/v/v); rotation speed: 900 rpm; flow rate: 2 mL/min; detection wavelength: 254 nm; stationary phase: upper phase; retention percentage of the stationary phase: 71.7%.

dramatically after the ethanol concentration exceeded 40% and peaked at 70% ethanol. After achieving optimal adsorption equilibrium, the adsorbate-laden column was eluted with 40% and 70% ethanol at a flow rate of 3 BV/h. As can be seen from Fig. 5C, the non-target components could be removed after elution with 40% ethanol of 3 BV, and the concentrations of target compounds in the effluent increased significantly. Subsequently, 70% ethanol of 8 BV can elute most of the target compounds adsorbed on the resin column. The optimal elution strategies were 3 BV of 40% ethanol and 8 BV of 70% ethanol, respectively. Therefore, the optimum enrichment and separation parameters for target compounds were as follows: feed volume of 3 BV, gradient elution of 3 BV of 40% ethanol and 8 BV of 70% ethanol. Under the above conditions, 10.31 g of enriched product was obtained in the scale-up experiment. After one run of AB-8 resin treatment, the contents of target compounds in the enriched product reached 0.15%, 0.11%, 0.51%, 0.31%, 5.52%, 4.09%, 6.82% and 0.56% with the recovery yields of 82.47%, 79.62%, 81.95%, 84.77%, 80.15%, 79.34%, 80.06% and 88.23%, which were 7.32–, 6.96-, 9.55-, 10.44-, 8.92-, 8.44-, 9.30- and 8.93-fold to those in crude extracts, respectively. It can be found that the target components can be easily and effectively enriched.

3.3. Selection of TPSS

A suitable TPSS is imperative to effectively separate target compounds by HSCCC. The K value is the most essential factor influencing the screening of the solvent system. The ideal K value should be in the range of 0.2–2.0 to get a satisfactory separation. A larger K value would result in prolonged retention time, inadequate resolution, and overly broad peaks, whereas a lower K value may be unable to separate adjacent compounds with poor peak resolution (Pan et al., 2020). This study investigated and determined the K values of different target chemicals in diverse hydrophilic and lipophilic TPSSs, as shown in Table 2. The polarity of target compounds in HMLF was moderate and the K values of the solvent system containing *n*-Butanol and $CHCl_3$ were excessively high. Thus, EtOAc-MeOH-H_2O (100:3:100, v/v/v) and Hex-EtOAc-MeOH-H_2O (1:5:1:5, v/v/v/v) with feasible K values and α were applied to separate target compounds from HMLF.

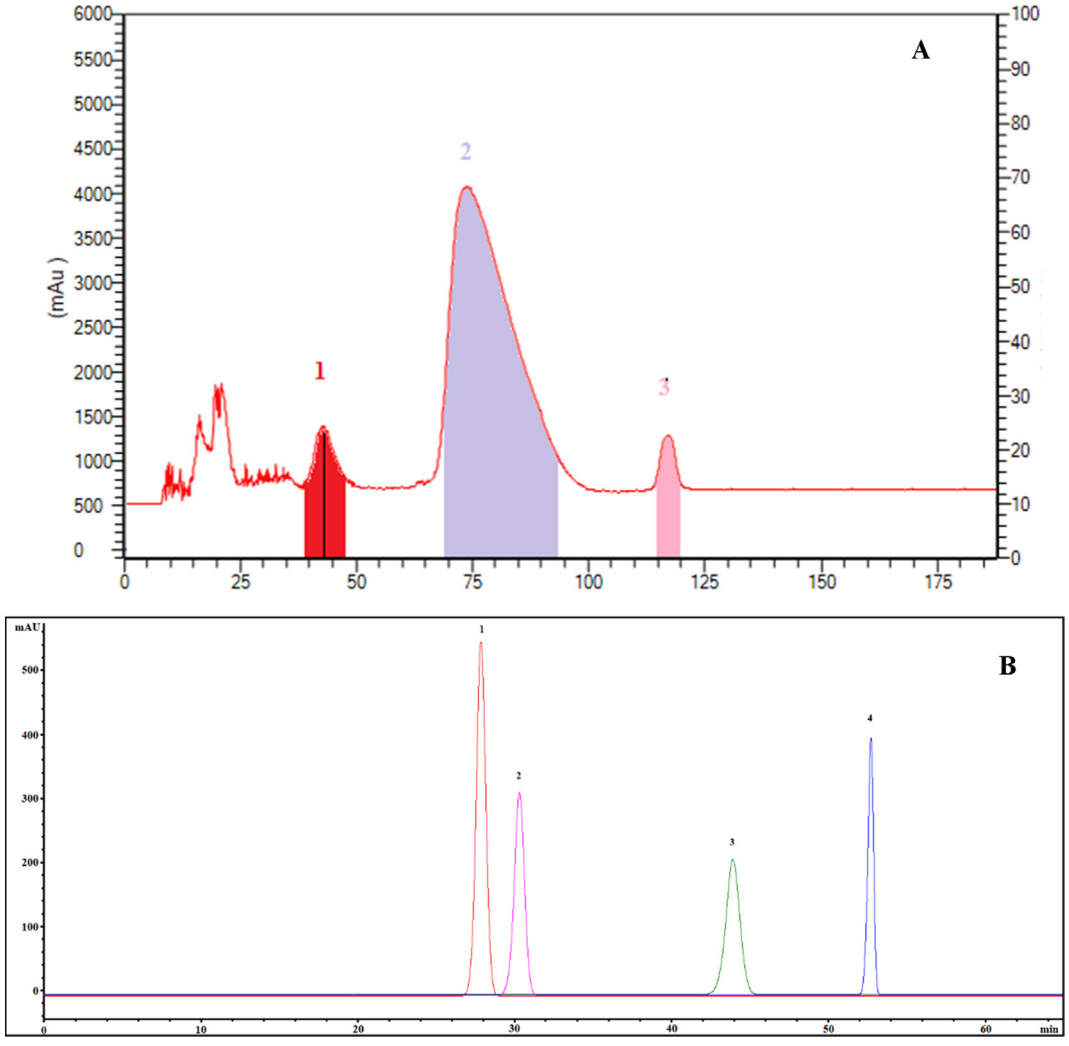

Fig. 7 HSCCC chromatogram of four target compounds isolated from HMLF (A) and HPLC chromatogram of four HSCCC fractions (B). 1, HY; 2, ISQ; 3, HI; 4, QOG. For HSCCC, solvent system: Hex-EtOAc-MeOH-H_2O (1:5:1:5, v/v/v/v); rotation speed: 850 rpm; flow rate: 2 mL/min; detection wavelength: 254 nm; stationary phase: upper phase; retention percentage of the stationary phase: 66.7%.

3.4. Purification and identification of target compounds

To accomplish the ideal separation of target compounds, the rotation speed should be high enough at a low mobile phase flow rate to enable for sufficient liquid–liquid extraction. The flow rate restricts the separation duration and quantity of stationary phase retained in the column, while low rotational speeds reduce the retention rate and extremely high rotational

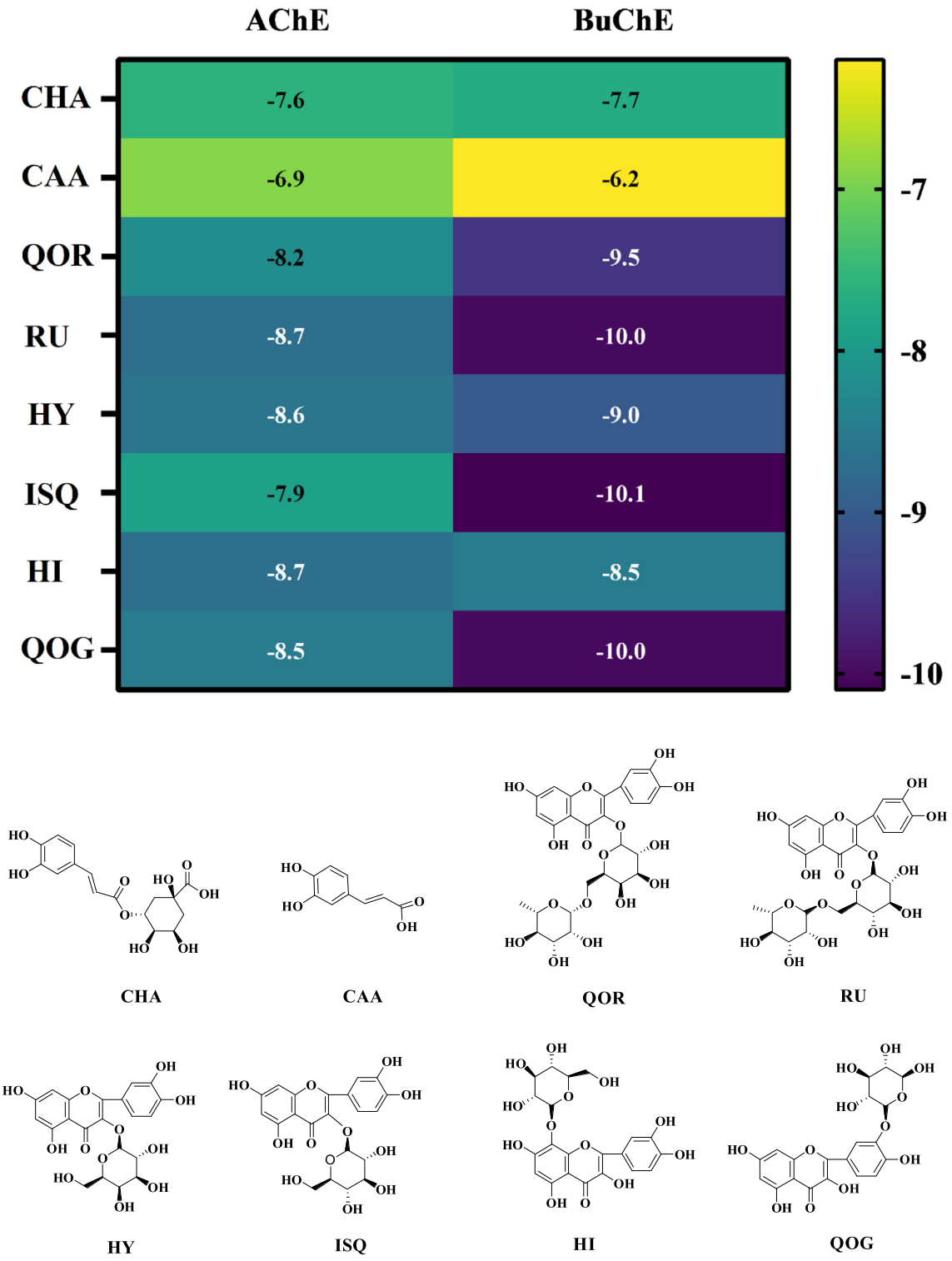

Fig. 8 The heatmap of the binding energy of isolated compounds (RU, HY, ISQ, QOR, CHA, CAA, HI and QOG) to AChE and BuChE and the 2D chemical structures of the ligands for molecular docking.

speeds widen the peaks owing to system vibration induced by the intense pulsing of the high pressure in the column (Li et al., 2022; Liu et al., 2022b). Five target compounds were separated and purified from 200 mg of the enriched product by HSCCC with the solvent system EtOAc-MeOH-H_2O (100:3:100, v/v/v) was performed at room temperature with a flow rate of 2 mL/min and a rotational speed of 900 rpm. The HSCCC chromatogram and the HPLC chromatogram of the five target compounds by HSCCC were demonstrated in Fig. 6. Subsequently, four target compounds were separated and purified from the enriched product by HSCCC with the solvent system Hex-EtOAc-MeOH-H_2O (1:5:1:5, v/v/v/v) at room temperature and a flow rate of 2 mL/min with a rotational speed of 850 rpm. The HSCCC chromatogram and the HPLC chromatogram of the four target compounds by HSCCC were demonstrated in Fig. 7. A total of 50.4 mg of target compounds were obtained from the eluent in a single run when combined with further crystallization. The final product purities were determined by HPLC to be > 95% by the peak area normalization method with recovery yields of 93.91%-98.02%.

The structural identification of the isolated compounds were performed and confirmed by ESI-MS/MS, FT-IR, ^{1}H and ^{13}C NMR spectra data in the analysis and by comparison with literature (Xu et al., 2022; Dall'Acqua et al., 2020; Santos et al., 2021) as shown in the Supporting information (Fig. S2-9). Ultimately, eight compounds obtained as chlorogenic acid (peak 1 in Fig. 6B, 3.2 mg, 96.91%), caffeic acid (peak 2 in Fig. 6B, 2.1 mg, 98.34%), quercetin-3-O-robibioside (peak 3 in Fig. 6B, 1.7 mg, 95.28%), rutin (peak 4 in Fig. 6B, 0.6 mg, 98.97%), hibifolin (peak 5 in Fig. 6B and peak 3 in Fig. 7B, 11.3 mg and 12.1 mg, 97.72%), hyperin (peak 1 in Fig. 7B, 10.4 mg, 98.04%), isoquercetin (peak 2 in Fig. 7B, 7.9 mg, 97.13%) and quercetin-3′-O-glucoside (peak 4 in Fig. 7B, 1.1 mg, 96.89%).

3.5. Molecular docking analysis of isolated compounds against acetylcholinesterase (AChE) and butyrylcholinesterase (BuChE)

The molecular docking analysis of the AChE and BuChE inhibitory potentials of eight isolated compounds was performed using AutoDock Vina. The isolated compounds showed binding affinities ranging from −6.9 to −8.7 kcal/mol against AChE, as displayed in Fig. 8. Among the eight isolated compounds, the highest binding affinity against AChE was recorded as −8.7 kcal/mol for RU and HI. Hydrogen bonds with Thr238, Arg296, Gln369, Asn533 and Ser541 (Fig. 9A, Table S2), hydrophobic interactions with Pro235, Pro312, Val367, Pro368, Val370, Trp532, Leu536, Pro537 and Leu540 (Fig. S9A) in molecular docking results of RU. Hydrogen bonds with Gly234, Pro235, Thr238, Gln369 and His405 (Fig. 9C, Table S2), hydrophobic interactions with Pro235, Pro312, Pro368, Val370, Pro410, Trp532, Leu536 and

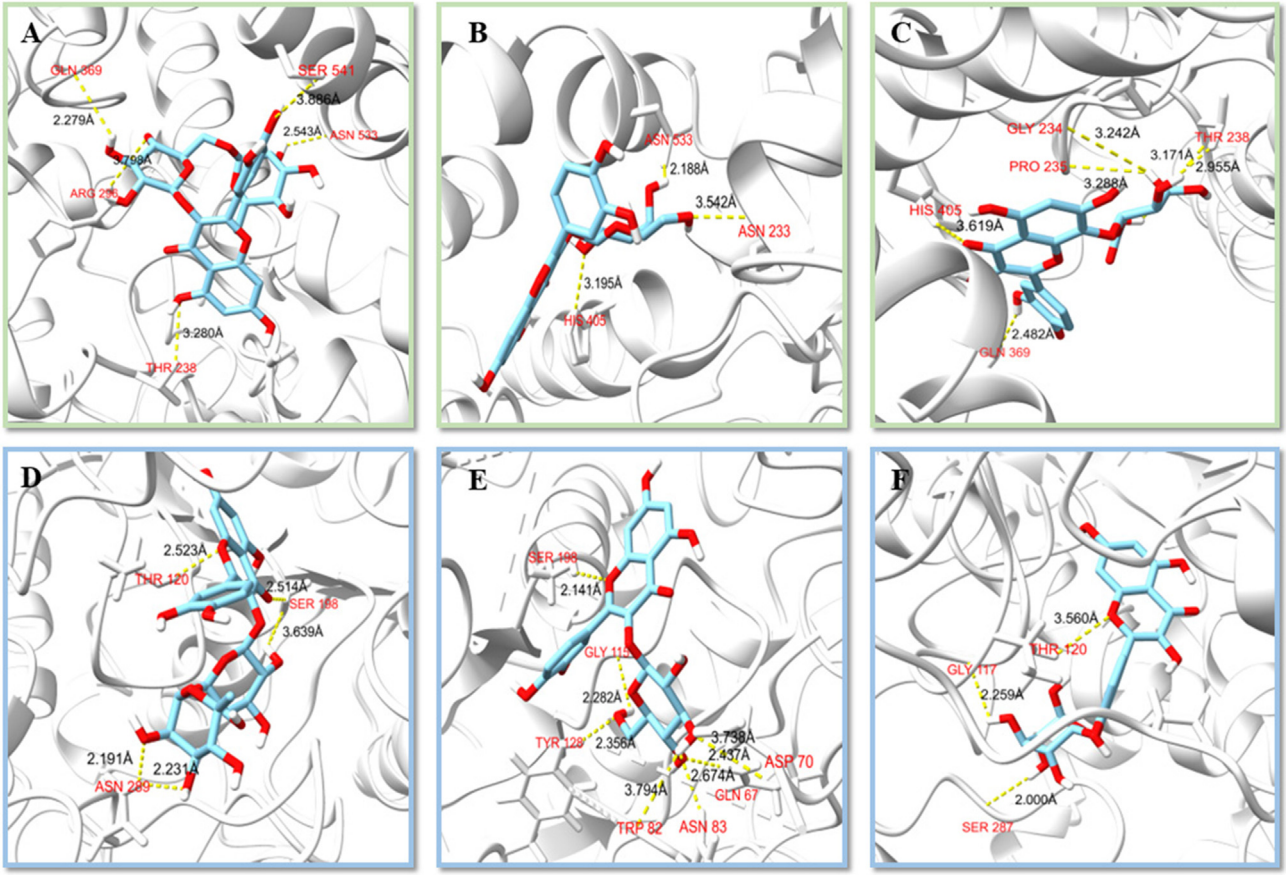

Fig. 9 Molecular interactions of isolated compounds against AChE (A-C) and BuChE (D-F). A, RU-AChE; B, HY-AChE; C, HI-AChE; D, QOR-BuChE; E, ISQ-BuChE; F, QOG-BuChE.

Leu540 were detected for HI (Fig. S10C). Notably, the oxygen atoms O5 and O13 of RU formed two polar bonds with two amino acid residues Gln369 and Thr238 of AChE, similar to HI. The interactions of the isolated compounds with BuChE were also analyzed, and it was calculated that the highest binding affinity with −10.0 kcal/mol for ISQ (Fig. 8). ISQ generated hydrogen bonds with Gln67, Asp70, Trp82, Asn83, Gly115, Tyr128 and Ser198 on BuChE (Fig. 9E), and hydrophobic interactions with Pro84, Tyr114, Leu125, Ala199, Trp231, Pro285, Leu286, Val288, Phe329, Phe398 and Ile442 (Fig. S10E). The location of ligands bound depends on Phe 329 and Tyr 332 of the E-helix, whose side chains project into the active site gorge (Darvesh et al., 2008). Phe329 appears to play an important role together with Trp231 in stabilizing an aromatic system in the groove of the acyl-binding pocket. It can be found that all the molecules interacted with AChE or BuChE in the same region. The main residues at the active site from AChE and BuChE for all the compounds and standards were noted to be Tyr, Trp, Ser, Phe and Trp, Tyr, His, Pro (Amjad et al., 2023). Inhibitors frequently used in the treatment of AD, such as Donepezil, Rivastigmine, and Galantamine were approved by the FDA. Combined with previous binding affinity data of these inhibitors against AChE and BuChE by many researchers (Table S4), it was found that the isolated RU, HI and ISQ had higher binding affinity than the drug molecules (Islam et al., 2013; Ghalloo et al., 2022). It was discovered through the examination of the isolated compounds' mechanism of binding inside the active sites of AChE and BuChE that the compounds fixed themselves inside the pocket by entwining numerous contacts (Larik et al., 2020). All of the data anticipated that the isolated compounds could have an inhibitory effect against AChE and BuChE. further predicted the possible inhibitory activity of the isolated compounds against AChE and BuChE.

4. Conclusion

Two phenolic acids (chlorogenic acid and caffeic acid) and six flavonoids (quercetin-3-O-robibioside, rutin, hyperin, isoquercetin, hibifolin and quercetin-3′-O-glucoside) were successfully separated and purified from *H. manihot* L. flower by HSCCC in conjunction with ultrasonic-assisted extraction and macroporous adsorption resin. After one run of AB-8 resin treatment, the contents of target compounds in enriched product reached 0.11–6.82%. In one cycle of separation procedure by HSCCC with a two-phase solvent system, and the purities of the eight target compounds were 95.28%-98.97%. The preparative throughout was up to 200 mg per cycle and the techniques were feasible for scaled-up production. Molecular docking revealed that the isolated polyphenols have distinct binding sites and energies towards AChE and BuChE, which may explain their potential neuroprotective activities. In recent years, many studies have reported the discovery of acetylcholine inhibitors from natural products, which have development potential in neurodegenerative diseases and AD (Moreira et al., 2022). These compounds have the following characteristics, which are composed of C, H, O and have benzene ring structure and multiple hydroxyl groups without N. Due to the structural particularities, these compounds have a strong antioxidant capacity and have significant effects on acetylcholine (Hwang et al., 2021). Taking polyphenols RU, HI and ISQ isolated in this study as examples, compared with previous studies, they have moderate molecular weights, more hydroxyl groups and stronger binding affinity. Due to the lack of N atoms, the binding affinity may not be advantageous compared to commercially available inhibitors, but as natural products, polyphenols tend to be less toxic and are not limited by hepatotoxicity profile and dosage frequency as Tacrine (Dilshad et al., 2022). The results indicated that the developed method was an effective strategy for the preparative separation of polyphenols from *H. manihot* L. flower. Furthermore, the technique combining the above two methods possessed wide application in natural products separation from plant herbs to obtain functional active ingredients used in the food and pharmaceutical industry.

CRediT authorship contribution statement

Ju-Zhao Liu: Funding acquisition, Investigation, Methodology, Validation, Writing – original draft. **Le-Le Wen:** Formal analysis, Methodology. **Xiao-Li Tian:** Methodology, Validation. **Yu-Jie Fu:** Conceptualization, Supervision. **Qi Cui:** Data curation, Formal analysis, Funding acquisition, Project administration, Supervision, Writing – review & editing.

Declaration of Competing Interest

The authors declare that they have no known competing financial interests or personal relationships that could have appeared to influence the work reported in this paper.

Acknowledgements

The authors gratefully acknowledge the financial support by China Postdoctoral Science Foundation (2021M692893, 2021M702927), National Natural Science Fund of China (82204552), Natural Science Foundation of Zhejiang Province (LQ22H280007), Research Project of Zhejiang Chinese Medical University (2022JKZKTS10), Zhejiang Province Traditional Chinese Medicine Science and Technology (2023ZR079, 2023ZR087), Traditional Chinese Medicine Modernization Special Project of Zhejiang Traditional Chinese Medicine Science and Technology Plan (2021ZX008). We appreciate the great experimental support from the Shanghai Qixia Technology Co., Ltd. and Public Platform of Medical Research Center, Academy of Chinese Medical Science, Zhejiang Chinese Medical University. We are also greatful to Mr. JinJin Yang from Maple Leaf School-Tianjin TEDA for his support in compouter technology.

Appendix A. Supplementary material

Supplementary data to this article can be found online at https://doi.org/10.1016/j.arabjc.2023.104791.

References

Alam, M., Ahmed, S., Elasbali, A.M., Adnan, M., Alam, S., Hassan, M.I., Pasupulet, V.R., 2022. Therapeutic implications of caffeic acid in cancer and neurological diseases. Front. Oncol. 12, 860508.

Albini, A., Festa, M.M.G., Ring, N., Baci, D., Rehman, M., Finzi, G., Sessa, F., Zacchigna, S., Bruno, A., Noonan, D.M., 2021. A polyphenol-rich extract of olive mill wastewater enhances cancer chemotherapy effects, while mitigating cardiac toxicity. Front. Pharmacol. 12, 694762.

Amjad, H., Abbasi, M.A., Sissiqui, S.Z., Iqbal, J., Rasool, S., Ashraf, M., Hussain, S., Shah, S.A.A., Imran, S., Shahid, M., Rasool, A., Rehman, M.T., ur Rehman, A., 2023. *In vitro* and *in silico* assessment of bioactivity properties and pharmacokinetic studies of new 3,5-disubstituted-1,2,4-triazoles. J. Mol. Struct. 1275, 134720.

Annunziata, G., Sureda, A., Orhan, I.E., Battino, M., Arnone, A., Jiménez-García, M., Capó, X., Cabot, J., Sanadgol, N., Giampieri, F., Tenore, G.C., Kashani, H.R.K., Silva, A.S., Habtemariam, S., Nabavi, S.F., Nabavi, S.M., 2021. The neuroprotective effects of polyphenols, their role in innate immunity and the interplay with the microbiota. Neurosci. Biobehav. R. 128, 437–453.

Christou, A., Stavrou, I.J., Kapnissi-Christodoulou, C.P., 2021. Continuous and pulsed ultrasound-assisted extraction of carob's antioxidants: Processing parameters optimization and identification of polyphenolic composition. Ultrason. Sonochem. 76, 105630.

Cui, Q., Liu, J.Z., Yu, L., Gao, M.Z., Wang, L.T., Wang, W., Zhao, X.H., Fu, Y.J., Jiang, J.C., 2020. Experimental and simulative studies on the implications of natural and green surfactant for extracting flavonoids. J. Clean. Prod. 274, 122652.

Dall'Acqua, S., Ak, G., Sut, S., Zengin, G., Yildiztugay, E., Mahomoodally, M.F., Sinan, K.I., Lobine, D., 2020. Comprehensive bioactivity and chemical characterization of the endemic plant *Scorzonera hieraciifolia* Hayek extracts: a promising source of bioactive compounds. Food Res. Int. 137, 109371.

Darvesh, S., Darvesh, K.V., McDonald, R.S., Mataija, D., Walsh, R., Mothana, S., Lockridge, O., Martin, E., 2008. Carbamates with differential mechanism of inhibition toward acetylcholinesterase and butyrylcholinesterase. J. Med. Chem. 51, 4200–4212.

Dermiki, M., Garrard, I.J., Jauregi, P., 2021. Selective separation of dyes by colloidal gas aphrons: Conventional flotation vs countercurrent chromatography. Sep. Purif. Technol. 279, 119770.

Dilshad, R., Khan, K.R., Ahmad, S., 2022. Phytochemical profiling, *in vitro* biological activities, and *in-silico* molecular docking studies of *Typha domingensis*. Arab. J. Chem. 15, (10) 104133.

Dvir, H., Silman, I., Harel, M., Rosenberry, T.L., Sussman, J.L., 2010. Acetylcholinesterase: From 3D structure to function. Chem Biol. Interact. 187 (1–3), 10–22.

Friesen, J.B., McAlpine, J.B., Chen, S.-N., Pauli, G.F., 2015. Countercurrent separation of natural products: an update. J. Nat. Prod. 78 (7), 1765–1796.

Gebicki, J.M., Nauser, T., 2021. Fast antioxidant reaction of polyphenols and their metabolites. Antioxidants 10 (8), 1297.

Ghalloo, B.A., Khan, K.U.R., Ahmad, S., Aati, H.Y., Al-Qahtani, J. H., Ali, B., Mukhtar, I., Hussain, M., Shahzad, M.N., Ahmed, I., 2022. Phytochemical profiling, *in vitro* biological activities, and *in silico* molecular docking studies of *Dracaena reflexa*. Molecules 27 (3), 913.

Gonzalez-Rivera, J., Mero, A., Husanu, E., Mezzetta, A., Ferrari, C., D'Andrea, F., Bramanti, E., Pomelli, C.S., Guazzelli, L., 2021. Combining acid-based deep eutectic solvents and microwave irradiation for improved chestnut shell waste valorization. Green Chem. 23 (24), 10101–10115.

Huang, P., Hong, J.X., Mi, J., Sun, B.L., Zhang, J.J., Li, C., Yang, W. E., 2022. Polyphenols extracted from *Enteromorpha clathrata* alleviates inflammation in lipopolysaccharide-induced RAW 264.7 cells by inhibiting the MAPKs/NF-κB signaling pathways. J. Ethnopharmacol. 286, 114897.

Hwang, J., Youn, K., Lim, G., Lee, J., Kim, D.H., Jun, M., 2021. Discovery of natural inhibitors of cholinesterases from *Hydrangea*: *In vitro* and *in silico* approaches. Nutrients 13 (1), 254.

Islam, M.R., Zaman, A., Jahan, I., Chakravorty, R., Chakraborty, S., 2013. *In silico* QSAR analysis of quercetin reveals its potential as therapeutic drug for Alzheimer's disease. J. Young Pharm. 5 (4), 173–179.

Jiang, Z.G., Wang, Y.H., Xiang, D., Zhang, Z.K., 2022. Structural properties, antioxidant and hypoglycemic activities of polysaccharides purified from pepper leaves by high-speed counter-current chromatography. J Funct Food. 89, 104916.

Jovanović, M., Mudrić, J., Drinić, Z., Matejić, J., Kitić, D., Bigović, D., Šavikin, K., 2022. Optimization of ultrasound-assisted extraction of bitter compounds and polyphenols from willow gentian underground parts. Sep. Purif. Technol. 281, 119868.

Larik, F.A., Saeed, A., Faisal, M., Hamdani, S., Jabeen, F., Channar, P.A., Mumtaz, A., Khan, I., Kazi, M.A., Abbas, Q., Hassan, M., Korabecny, J., Seo, S.Y., 2020. Synthesis, inhibition studies against AChE and BChE, drug-like profiling, kinetic analysis and molecular docking studies of N-(4-phenyl-3-aroyl-2(3H)-ylidene) substituted acetamides. J. Mol. Struct. 1203, 127459.

Li, H., Guo, H., Luo, Q., Wu, D.T., Zou, L., Liu, Y., Li, H.B., Gan, R.Y., 2021. Current extraction, purification, and identification techniques of tea polyphenols: An updated review. Crit. Rev. Food Sci. Nutr., 1–19

Li, L.X., Zhao, J., Yang, T.T., Sun, B.H., 2022. High-speed countercurrent chromatography as an efficient technique for large separation of plant polyphenols: A review. Food Res. Int. 153, 110956.

Liang, Q., Zhang, J.S., Su, X.G., Meng, Q.W., Dou, J.P., 2019. Extraction and separation of eight ginsenosides from flower buds of *Panax Ginseng* using aqueous ionic liquid-based ultrasonic-assisted extraction coupled with an aqueous biphasic system. Molecules. 24 (4), 778.

Lin, Y.L., Han, C., Xu, Q.Q., Wang, W.L., Li, L.N., Zhu, D.R., Luo, J.G., Kong, L.Y., 2020. Integrative countercurrent chromatography for the target isolation of lysine-specific demethylase 1 inhibitors from the roots of *Salvia miltiorrhiza*. Talanta 206, 120195.

Liu, J.Z., Lyu, H.C., Fu, Y.J., Cui, Q., 2022b. *Amomum tsao-ko* essential oil, a novel anti-COVID-19 Omicron spike protein natural products: A computational study. Arab J Chem. 15, 103916.

Liu, Y., Kong, K.W., Wu, D.T., Liu, H.Y., Li, H.B., Zhang, J.R., Gan, R.Y., 2022c. Pomegranate peel-derived punicalagin: Ultrasonic-assisted extraction, purification, and its alpha-glucosidase inhibitory mechanism. Food Chem. 374, 131635.

Liu, J.Z., Lyu, H.C., Fu, Y.J., Jiang, J.C., Cui, Q., 2022a. Simultaneous extraction of natural organic acid and flavonoid antioxidants from *Hibiscus manihot* L. flower by tailor-made deep eutectic solvent. LWT-Food. Sci. Technol. 163, 113533.

Moreira, N.C.S., Tamarozzi, E.R., Lima, J.E.B.F., Piassi, L.D.O., Carvalho, I., Passos, G.A., Sakamoto-Hojo, E.T., 2022. Novel dual AChE and ROCK2 inhibitor induces neurogenesis via PTEN/AKT pathway in Alzheimer's disease model. Int J. Mol. Sci. 23 (23), 14788.

Pan, Z.H., Ning, D.S., Fu, Y.X., Li, D.P., Zou, Z.Q., Xie, Y.C., Yu, L. L., Li, L.C., 2020. Preparative isolation of piceatannol derivatives from Passion fruit (*Passiflora edulis*) seeds by high-speed countercurrent chromatography combined with high-performance liquid chromatography and screening for alpha-glucosidase inhibitory activities. J. Arg. Food Chem. 68 (6), 1555–1562.

Périno-Issartier, S., Abert-Vian, M., Chemat, F., 2011. Solvent free microwave-assisted extraction of antioxidants from sea buckthorn (*Hippophae rhamnoides*) food by-products. Food Bioprocess Technol. 4, 1020–1028.

Razmi, B., Ghasemi-Fasaei, R., Ronaghi, A., Mostowfizadeh-Ghalamfarsa, R., 2022. Application of Taguchi optimization for evaluating the capability of hydrochar, biochar, and activated carbon prepared from different wastes in multi-elements bioadsorption. J. Clean. Prod. 347, 131292.

Rosenberry, T.L., Brazzolotto, X., Macdonald, I.R., Wandhammer, M., Trovaslet-Leroy, M., Darvesh, S., Nachon, F., 2017. Comparison of the binding of reversible inhibitors to human butyrylcholinesterase and acetylcholinesterase: A crystallographic, kinetic and calorimetric study. Molecules. 22 (12), 2098.

Santos, A.L., Soares, M.G., de Medeiros, L.S., Ferreira, M.J.P., Sartorelli, P., 2021. Identification of flavonoid-3-O-glycosides from leaves of *Casearia arborea* (Salicaceae) by UHPLC-DAD-ESI-HRMS/MS combined with molecular networking and NMR. Phytochem Analysis. 32 (6), 89–898.

Socała, K., Szopa, A., Serefko, A., Poleszak, E., Wlaź, P., 2021. Neuroprotective effects of coffee bioactive compounds: A review. Int. J. Mol. Sci. 22 (1), 107.

Song, X.Y., Li, K., Cui, L., Yu, J.Q., Ali, I., Zhu, H., Wang, Q.Q., Wang, X., Wang, D.J., 2020. A simple and efficient linear gradient coupled with inner-recycling high-speed counter-current chromatography mode for the preparative separation of flavonoid glycosides from leaves of custard apple. J. Chromatogr. A. 1615, 460719.

Souadia, A., Gourine, N., Yousfi, M., 2022. Optimization total phenolic content and antioxidant activity of *Saccocalyx satureioides* extracts obtained by ultrasonic-assisted extraction. J Chemometr. 36 (7), e3428.

Sridhar, A., Ponnuchamy, M., Kumar, P.S., Kapoor, A., Vo, D.V.N., Prabhakar, S., 2021. Techniques and modeling of polyphenol extraction from food: a review. Environ Chem. Lett. 19 (4), 3409–3443.

Tan, J.Q., Cui, P.S., Ge, S.Q., Cai, X., Li, Q., Xue, H.K., 2022. Ultrasound assisted aqueous two-phase extraction of polysaccharides from *Cornus officinalis* fruit: Modeling, optimization, purification, and characterization. Ultrason Sonochem. 84, 105966.

Temerk, Y., Ibrahim, H., 2016. Fabrication of a novel electrochemical sensor based on Zn–In_2O_3 nanorods coated glassy carbon microspheres paste electrode for square wave voltammetric determination of neuroprotective hibifolin in biological fluids and in the flowers of *hibiscus vitifolius*. J. Electroanal Chem. 782, 9–18.

Vrabec, R., Maříková, J., Ločárek, M., Korábečný, J., Hulcová, D., Hošťálková, A., Kuneš, J., Chlebek, J., Kučera, T., Hrabinová, M., Jun, D., Soukup, O., Andrisano, V., Jenčo, J., Šafratová, M., Nováková, L., Opletal, L., Cahlíková, L., 2022. Monoterpene indole alkaloids from *Vinca minor* L. (Apocynaceae): Identification of new structural scaffold for treatment of Alzheimer' s disease. Phytochemistry. 194, 113017.

Wang, D., Zhao, H., Zhu, H., Wen, L., Yu, J., Li, L., Chen, L., Geng, Y., 2019. A novel method for highly efficient biotransformation and separation of isoflavone aglycones from soybean with high-speed counter-current chromatography. Ind. Crop. Prod. 129, 224–230.

Wu, W.X., Jiang, S., Liu, M.M., Tian, S.G., 2021. Simultaneous process optimization of ultrasound-assisted extraction of polyphenols and ellagic acid from pomegranate (*Punica granatum* L.) flowers and its biological activities. Ultrason Sonochem. 80, 105833.

Xu, Y., Zhang, J., Pan, T., Ren, F.Z., Luo, H.L., Zhang, H., 2022. Synthesis, characterization and effect of alkyl chain unsaturation on the antioxidant activities of chlorogenic acid derivatives. LWT-Food Sci. Technol. 162, 113325.

Xu, H., Zhou, Q., Liu, B., Cheng, K.W., Chen, F., Wang, M.F., 2021. Neuroprotective potential of Mung bean (*Vigna radiata* L.) polyphenols in Alzheimer's disease: A review. J. Arg Food Chem. 69 (39), 11554–11571.

Xue, H.K., Tan, J.Q., Zhu, X.H., Li, Q., Tang, J.T., Cai, X., 2021. Counter-current fractionation-assisted and bioassay-guided separation of active compounds from cranberry and their interaction with alpha-glucosidase. LWT-Food Sci. Technol. 145, 111374.

Yang, J., Li, N.N., Wang, C.Y., Chang, T., Jiang, H.C., 2021. Ultrasound-homogenization-assisted extraction of polyphenols from coconut mesocarp: Optimization study. Ultrason Sonochem. 78, 105739.

Yang, Y., Meng, J., Li, H.Q., Gu, D.Y., Wang, S., He, S., Xu, H.Y., Ito, Y., 2020. Elution-extrusion and back-extrusion counter-current chromatography using three-phase solvent system for separation of organic dye mixture. Sep. Purif. Technol. 248, 117024.

Zhang, Y.C., Liu, C.M., Li, S.N., Hou, W.C., Tsao, R., 2021. Development of ultrasound-assisted centrifugal extraction and online solvent concentration coupled with parallel countercurrent chromatography for the preparation of purified phytochemicals: Application to *Lycium ruthenicum*. Ind. Crop. Prod. 162, 113266.

Zhu, J.T.T., Choi, R.C.Y., Chu, G.K.Y., Cheung, A.W.H., Gao, Q.T., Li, J., Jiang, Z.Y., Dong, T.T.X., Tsim, K.W.K., 2007. Flavonoids possess neuroprotective effects on cultured pheochromocytoma PC12 cells: a comparison of different flavonoids in activating estrogenic effect and in preventing beta-amyloid-induced cell death. J. Agric. Food Chem. 55 (6), 2438–2445.

Zhu, J.T.T., Choi, R.C.Y., Xie, H.Q., Zheng, K.Y.Z., Guo, A.J.Y., Bi, C.W.C., Lau, D.T.W., Li, J., Dong, T.T.X., Lau, B.W.C., Chen, J. J., Tsim, K.W.K., 2009. Hibifolin, a flavonol glycoside, prevents β-amyloid-induced neurotoxicity in cultured cortical neurons. Neurosci Lett. 461, 172–176.

Zuo, G., Wang, Z., Quispe, Y.N.G., Hwang, S.H., Kim, H.Y., Kang, B.G., Lim, S.S., 2019. Target guided isolation of potential tyrosinase inhibitors from *Otholobium pubescens* (Poir.) J.W. Grimes by ultrafiltration, high-speed counter-current chromatography and preparative HPLC. Ind. Crop. Prod. 134, 195–205.